Bioorganic & Medicinal Chemistry 16 (2008) 9106–9112

Contents lists available at ScienceDirect

Bioorganic & Medicinal Chemistry

journal homepage: www.elsevier.com/locate/bmc

Spectroscopic studies on the formation and thermal stability of DNA triplexes with a benzoannulated δ-carboline–oligonucleotide conjugate

Andrea Eick [a], Zhou Xiao [a], Peter Langer [b], Klaus Weisz [a,*]

[a] Institut für Biochemie, Ernst-Moritz-Arndt-Universität Greifswald, Felix-Hausdorff-Str. 4, D-17487 Greifswald, Germany
[b] Institut für Chemie, Universität Rostock, Albert-Einstein-Str. 3a, 18059 Rostock, Germany

ARTICLE INFO

Article history:
Received 11 June 2008
Revised 2 September 2008
Accepted 10 September 2008
Available online 13 September 2008

Keywords:
DNA triplex
δ-Carboline
Oligonucleotide conjugate
Spectroscopy

ABSTRACT

A benzoannulated δ-carboline with a phenyl substituent has been covalently tethered to the 3′-end of a triplex-forming oligonucleotide and its ability to bind and stabilize DNA triple helices has been examined by various spectroscopic methods. UV thermal melting experiments were conducted with different hairpin duplexes and with a complementary single-stranded oligonucleotide as targets for the conjugate. The δ-carboline ligand preferentially binds triplexes over duplexes and leads to a temperature increase of the triplex-to-duplex transition by up to 23 °C. The results obtained from UV, CD and fluorescence measurements suggest that the δ-carboline ligand exhibits specific interactions with a triplex and favors binding by intercalation at the triplex–duplex junction.

1. Introduction

Triple helix formation through the sequence-specific recognition of a double-helical DNA target by a third strand oligonucleotide (TFO) has long been recognized as a potentially powerful tool for numerous applications in medicine and molecular biology. These include the control of gene expression,[1,2] site-directed mutagenesis[3,4] or mapping of genomic DNA.[5,6] The TFO in such triplexes binds in the major groove of double-helical DNA forming specific hydrogen bonds to purine bases on one of the two strands. In general, two types of triple helices have been characterized depending on the orientation of the third strand. In the pyrimidine motif, a homopyrimidine strand binds to a homopurine sequence of the duplex DNA in a parallel orientation with the formation of T·AT and C^+·GC triplets. Because cytosine bases in the third strand have to be protonated in order to form two Hoogsteen hydrogen bonds to a guanine base, a low pH value is generally required for stable triplex formation. In a second triplex motif, a purine third strand binds in an antiparallel orientation with respect to the oligopurine tract of the underlying duplex forming G·GC and A·AT triplets through reverse Hoogsteen hydrogen bonds. In addition, triplex forming oligonucleotides composed of T and G may also bind to a homopurine stretch of double-helical DNA with an orientation that depends upon the particular base sequence [for a review, see Ref. 7].

Presently, a more widespread use of triplex formation through the recognition of double-stranded nucleic acids by oligonucleotides is often hampered by the low stability of the formed triple-helical complexes, especially under physiological conditions. Strategies to enhance triplex stability have thus emerged as one of the major challenges towards more general future applications [for a review, see Ref. 8]. In addition to various chemical modifications of backbone, bases and sugar residues, additional stacking interactions through molecular capping of nucleic acid bases by aromatic and polycyclic compounds, that are either covalently linked to the 3′- or 5′-terminus of the TFO,[9–11] attached at an internucleotide position[12–14] or being part of a linker region in an intramolecular construct,[15–17] have been exploited for triplex stabilization. Some of these moieties may also serve as probes for triplex formation, for example, through changes of their fluorescence properties upon binding of the conjugate to the target duplex. Whereas a large number of natural and synthetic drugs have been shown to bind and stabilize nucleic acid structures, only a limited number of compounds have been found to selectively bind triplexes. The latter include annelated quinolizinium salts,[18,19] benzopyridoindole (BPI) and benzopyridoquinoxaline (BPQ) derivatives,[20,21] dibenzophenanthrolines,[22] 2-naphthyl substituted quinolines[23] and substituted anthraquinones.[24] We have recently shown in preliminary studies, that a novel phenyl-substituted benzoannulated δ-carboline, 5-phenyl-6*H*-indolo[3,2-*b*]quinoline, when tethered to a third strand oligonucleotide is effective in stabilizing DNA triplexes formed with a cognate duplex.[25] In the present work, we have continued studies on the ligand binding and thermal stability of triple helices formed by a δ-carboline–TFO conjugate and various double-helical DNA targets through UV, CD and fluorescence measurements. Also, full experimental details of the ligand-oligonucleotide coupling reaction, that provides the conjugates in good yields, are reported.

* Corresponding author. Tel.: +49 (0)3834 864426; fax: +49 (0)3834 864427.
E-mail address: weisz@uni-greifswald.de (K. Weisz).

0968-0896/$ - see front matter © 2008 Elsevier Ltd. All rights reserved.
doi:10.1016/j.bmc.2008.09.026

2. Results and discussion

2.1. UV melting experiments

Conjugation of the phenyl-substituted benzoannulated δ-carboline to the 3′-terminus of an oligonucleotide was accomplished through the coupling of the NHS-activated ligand with the 3′-aminoalkyl-modified oligonucleotide synthesized by standard protocols from FMOC-protected C7 amino link solid support.[25] After a reaction time of 5 days at elevated temperatures in a two-phase DMF-phosphate buffer system, the coupled product was isolated and subjected to a final HPLC purification. To promote dissolution of the NHS ester in the solvent system, lithium chloride was used as an additive for the coupling reaction giving a final yield of ⩾50% for the purified product.

Temperature-dependent UV measurements were performed on various triplexes formed by the δ-carboline–oligonucleotide conjugate and hairpin duplexes with 10 base pairs each (see Fig. 1). Triplex formation with an intramolecularly folded and thus entropically stabilized hairpin duplex ensures two well-separated transitions for double-helix denaturation at high temperatures and third-strand dissociation at much lower temperatures associated with a hyperchromicity at 260 nm. As shown by the UV melting curves in Figure 2, triplex **Trip1** showed a significant increase in the triplex-to-duplex melting temperature ΔT_{m1} of 22 °C when compared to the unmodified triplex reference, indicating strong interactions of the attached polycyclic δ-carboline with the triple-helical structure. Additionally, when the corresponding δ-carboline absorbance at 350 nm is recorded as a function of temperature, a single cooperative transition at the triplex–duplex melting temperature T_{m1} with an associated hypochromism of 33% upon triplex formation is found and suggests, that the dissociation of the conjugated third strand from the duplex occurs by a one-step process (not shown).

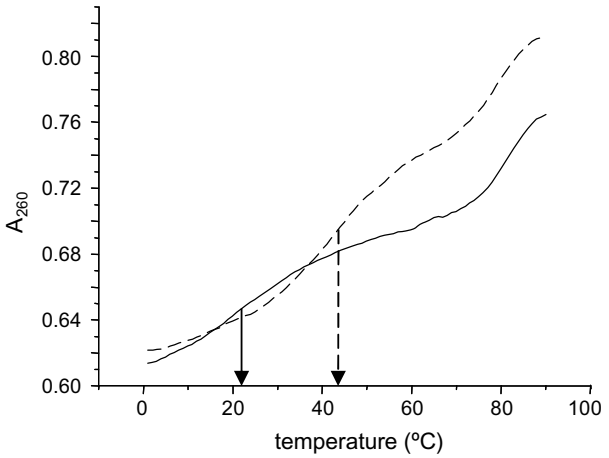

Figure 2. UV melting curves measured at 260 nm for the non-conjugated reference (solid line) and for the conjugate triplex **Trip1** (broken line). T_{m1} values as determined from the maxima of the first derivative plots are indicated by the vertical arrows.

In contrast, a smaller ligand-induced stabilization is observed for a duplex **Dup1** formed by the hybridization of the TFO with a

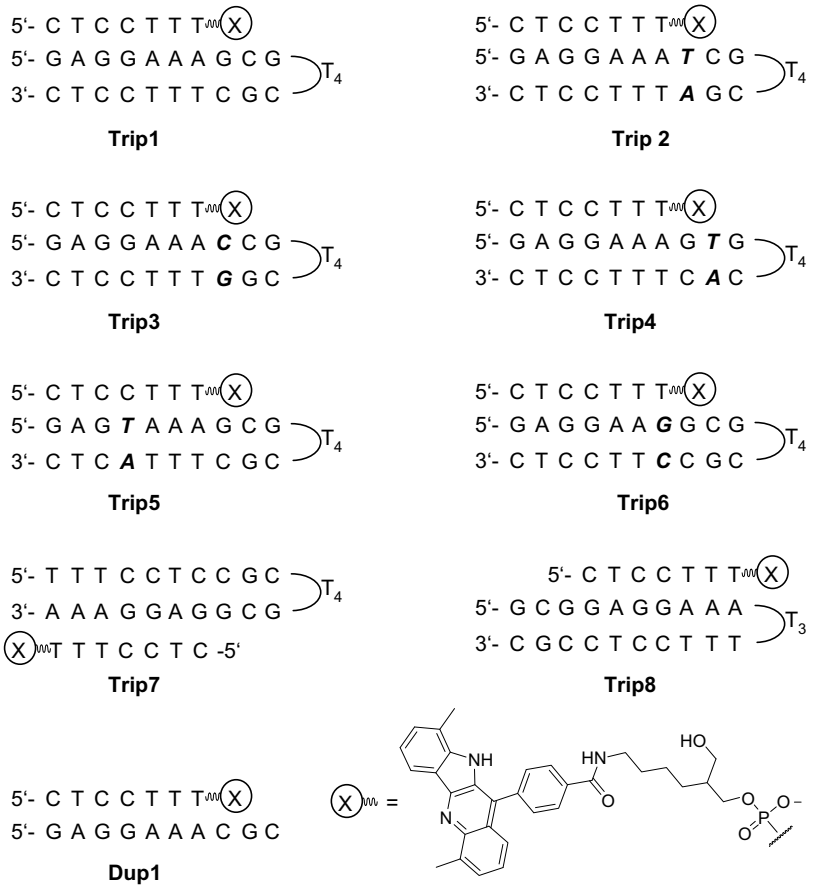

Figure 1. Triplex constructs with the TFO conjugate used in this study. The conjugate with the 3′-linked ligand X runs parallel to the purine stretch of the target hairpin duplex. Single base pair substitutions in triplexes **Trip2-6** are marked by bold letters.

single-stranded 10 mer target possessing a complementary purine sequence (see Fig. 1). Under the same buffer conditions and pH 5, ligand binding within the double-helical structure results in a much smaller increase of the duplex melting temperature by 11 °C consistent with a noticeably weaker affinity of the ligand towards the duplex (Table 1). Interestingly, the ligand-induced thermal duplex stabilization was found to be strongly affected by the pH and ΔT_m for the duplex melting is further reduced to only +4 °C at pH 7. It must be stressed, that relative changes in melting temperatures do not necessarily translate into relative binding constants due to the temperature dependence of association. However, because melting of both double- and triple-helical systems formed upon hybridization with the conjugate occurs within a sufficiently narrow temperature range, these temperature dependencies can mostly be neglected and differences in thermal stabilizations can be used as a reasonable measure of relative binding affinities in the present case.

As seen from Table 1, base pair substitutions in the duplex overhang of **Trip1** to form constructs **Trip2–4** only result in minor changes of the ligand-induced triplex stabilization. Whereas a base pair replacement at the center of the duplex overhang does not affect the ligand binding (**Trip4**), base pair substitutions at the triplex–duplex junction are associated with a small decrease in triplex stabilization (see **Trip2** and **Trip3**). Based on the larger ΔT_{m1} for **Trip1** and **Trip4**, a modest preference of the ligand for the purine sequence (AG)·(CT) in the duplex target at the triplex–duplex junction can be derived. Note, however, that a noticeable decrease of the triplex melting temperature associated with a (AG)·(CT) to (AC)·(GT) substitution at the junction of **Trip3** is also observed for the corresponding reference sample and points to a structural change that may affect the adjacent triplex region and leads to a general weakening of the TFO binding. To position the ligand away from the triplex–duplex junction, **Trip7** and **Trip8** were constructed with the δ-carboline facing the triplex blunt end. Although a considerable increase in ΔT_{m1} indicates significant triplex stabilization by the δ-carboline, the stabilizing effect is about equally reduced for both constructs by 6–8 °C compared to the parent triplex **Trip1** with the ligand facing the triplex–duplex junction. The tight T3 miniloop in **Trip8** does not favor specific interactions with the ligand and prevents its external stacking on the terminal base triplet.[26,27] On the other hand, the flexible linker of the conjugate allows the ligand to easily fold back into the 5′-direction and consequently intercalation between two base triplets is expected to be the major binding mode for both **Trip7** and **Trip8**.

Table 1
UV melting temperatures of triple- and double-helical constructs[a]

Triplex/duplex	T_{m1} (°C) triplex–duplex	T_{m2} (°C) duplex–single strand	ΔT_{m1} (°C) triplex–duplex
Trip1	44 (22)	79 (81)	22
Trip2	41 (21)	77 (76)	20
Trip3	38 (18)	80 (81)	20
Trip4	45 (22)	74 (74)	23
Trip5	– (–)[b]	75 (75)	–
Trip6	31 (15)	82 (81)	16
Trip7	41 (25)	80 (82)	16
Trip8	45 (31)	80 (78)	14
Dup1	–	25 (14)	11[c]
Dup1[d]	–	18 (14)	4[c]

Values for underivatized reference samples are given in parentheses.
[a] Uncertainty in $T_m \leqslant 1$ °C.
[b] Not observed.
[c] ΔT_{m2} (°C) for duplex–single strand transition.
[d] 20 mM phosphate, 100 mM NaCl, pH 7.

A single mismatch within the center of the triplex stem is not tolerated and no triplex formation with the unmodified TFO or the TFO conjugate could be detected for **Trip5**. These results show that the binding affinity of the ligand does not significantly compromise the sequence specificity of the TFO towards its cognate sequence and one central mismatch prevents binding of the 7mer conjugate to its target. In contrast, a mismatch at the terminal base triad as introduced into construct **Trip6** is less destabilizing allowing the formation of a triplex even with the unmodified ligand-free TFO. Stabilization of the conjugate triplex **Trip6** amounts to a ΔT_{m1} of 16 °C. The smaller stabilization compared to triplex **Trip1** indicates that the δ-carboline binding is weakened due to this change in the base sequence. This again suggests direct interactions of the δ-carboline with the terminal base triplet at the triplex–duplex junction that might be hampered by the distorted geometry of the mismatched base triad.

The interaction of the δ-carboline within a triple helix was also monitored by spectrophotometric titrations of a conjugate buffer solution with the target duplex to form **Trip1**. As shown in Figure 3, the oligonucleotide-linked ligand exhibits two intense absorption bands at 350 nm and at 377 nm. The titration of double-stranded DNA induces significant perturbations in the two spectral bands. In contrast to the absorption maximum at 350 nm, the long-wavelength absorption band at 377 nm

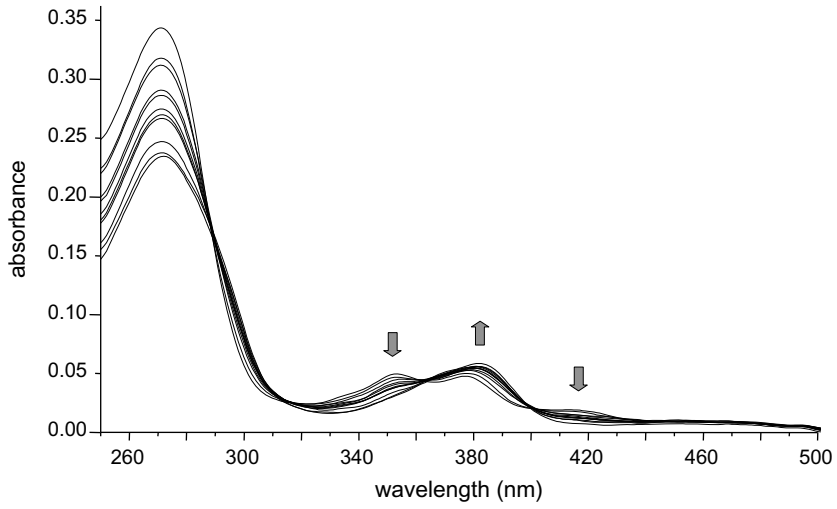

Figure 3. Absorption spectra of a 3.6 μM solution of oligonucleotide conjugate and increasing amounts (0–7.2 μM) of complementary double-stranded oligonucleotide at 20 °C; arrows indicate the development of the absorption bands upon DNA titration.

exhibits an increase in intensity together with a bathochromic shift of 5 nm relative to the free conjugate upon triplex formation with the target duplex. Moreover, several isosbestic points within the absorption region of the ligand clearly support the presence of only two spectrally distinct species of the δ-carboline chromophore upon triplex formation and provide evidence that one binding mode is adopted almost exclusively within the triple-helical complex.

2.2. Circular dichroism

Temperature-dependent CD experiments were employed on **Trip1** to independently probe structural changes for the nucleic acid and the δ-carboline upon triplex formation. Figure 4 shows corresponding CD spectra of the triple-helical complex in a temperature range from 20 °C to 60 °C. The high-temperature spectra with a positive CD band at 280 nm and a negative CD band near 250 nm equal summed spectra of the conjugate and the target duplex in line with a dissociated third strand oligonucleotide and a free B-type hairpin DNA (not shown). In contrast, formation of a triple-helical complex at 20 °C is indicated by a more negative CD band at around 250 nm and in particular by an intense negative short-wavelength band at around 210 nm.[28] Another weak negative CD band, centered at the long-wavelength absorbance maximum of the δ-carboline at 380 nm and fully reproduced by an independent series of temperature-dependent experiments, is only observed for the triple-helical complex at lower temperatures and disappears at about 50 °C after triplex melting (see inset Fig. 4). It demonstrates that the ligand is bound to an asymmetric environment and coupling between the transition dipoles of the ligand chromophore and DNA results in an induced CD (ICD) for the DNA-bound δ-carboline moiety. The sign of the ICD depends upon the specific ligand orientation within the complex through its transition dipole moment for the electronic transition and in line with its structural resemblance to other typical intercalators, a weak negative ICD of the δ-carboline–TFO conjugate when adding a duplex target may be taken as evidence for an intercalative mode of binding.[29]

2.3. Fluorescence measurements

In static fluorescence measurements, the maxima in excitation and emission wavelengths of the δ-carboline in the unbound conjugate and in a triple-helical complex were determined above 300 nm to exclude any masking effect by the nucleic acid bases. Whereas the excitation wavelength of the δ-carboline did not change upon triplex formation with the duplex target (λ_{ex} = 350 nm), the emission wavelength shifted from λ_{em} = 466 nm for the free conjugate to λ_{em} = 463 nm for the triple-helical complex. Such a hypsochromic shift in the fluorescence emission is typical for a change to a less polar environment and is likely to reflect the ligand binding associated with protection from the aqueous environment.

To examine the influence of triplex formation on the fluorescence intensity of the δ-carboline, temperature-dependent measurements of a 1:1 mixture of the conjugate and the target duplex were performed. The sample was excited at 350 nm and the emission was monitored between 360 and 600 nm in a temperature range between 20 °C and 80 °C. As shown in Figure 5, the fluorescence intensity increases with increasing temperature and reaches the same value at higher temperatures that is observed for the free conjugate at corresponding temperatures. In addition, a shift in the emission wavelength from 463 nm at 20 °C to 466 nm at 50 °C is again observed indicating, that the conjugate with the δ-carboline is dissociated from the target duplex above 50 °C. Plotting the fluorescence intensity at 466 nm against the temperature gives a transition temperature of 44 °C in agreement with the UV melting data, again indicating a one-step dissociation of the δ-carboline–TFO conjugate from the duplex (see inset Fig. 5). Consequently, the observed hypochromic effect with significant quenching of ligand fluorescence below 50 °C must be attributed to triplex formation and the binding of the δ-carboline to the DNA. At 20 °C the fluorescence intensity of the bound δ-carboline is approximately 13 times lower compared to the fluorescence emission of the conjugate pointing to strong electronic interactions between the ligand and DNA bases. Note that the effect of increasing temperature on the fluorescence intensity of the free conjugate

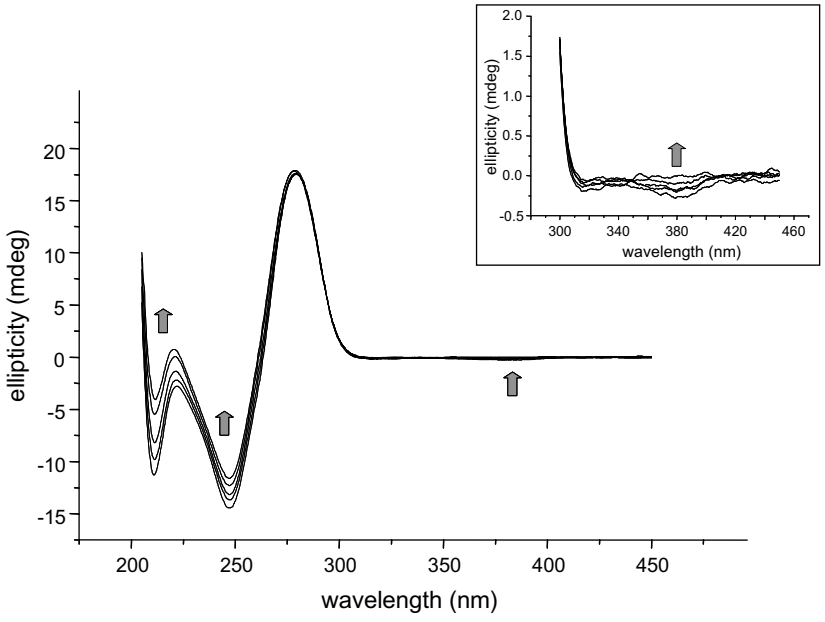

Figure 4. Circular dichroism spectra for the conjugate triplex **Trip1** at 20 °C, 30 °C, 40 °C, 50 °C and 60 °C; arrows indicate the spectral changes with increasing temperature. The inset shows an expansion of the spectral region comprising the maximum of ligand absorbance at 380 nm.

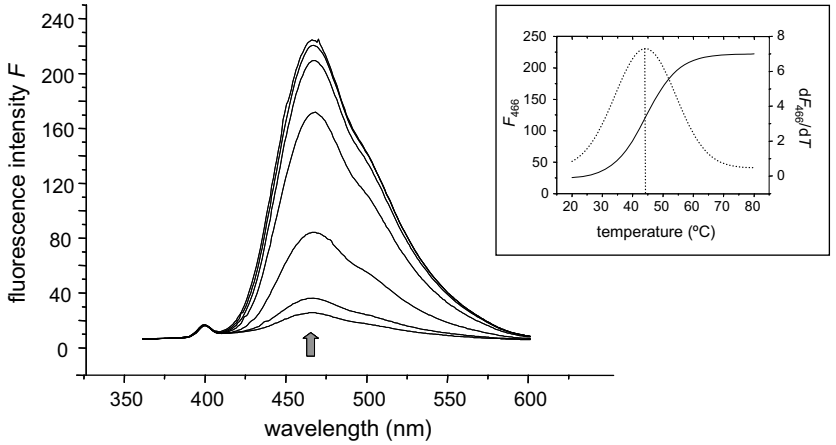

Figure 5. Fluorescence emission spectra for the conjugate triplex **Trip1** at 20 °C, 30 °C, 40 °C, 50 °C, 60 °C, 70 °C and 80 °C; the arrow indicates the spectral changes with increasing temperature. The inset shows the fluorescence melting curve at 466 nm together with its first derivative.

is small in comparison to the effect observed for the ligand binding to the triple-helical complex (not shown).

2.4. Ligand binding

Differences in the ligand-mediated thermal stabilization as observed for triplexes **Trip1**–**4** with the δ-carboline positioned at the triplex–duplex junction and for triplexes **Trip7** and **Trip8** with the ligand positioned at the triplex blunt end may be attributed to δ-carboline–DNA interactions of different strength and point to the triplex–duplex junction as being the favorable intercalation site for the ligand. In fact, triplex–duplex junctions have been shown in the past to be strong binding sites for various intercalators and this has been ascribed to some structural distortions inherent to the junction.[30,31] It has to be noted, that due to the short triple helix with only seven base triplets comprising pH-dependent C^+·GC triads, triplexes had to be stabilized by a low pH and by the addition of spermine for reliable measurements in the accessible temperature range. As suggested by the pH dependent thermal stabilization of the duplex in the presence of the δ-carboline, the pyrido ring nitrogen of our ligand may partially undergo protonation/deprotonation between pH 5 and 7. Because a positive charge promotes interactions with a highly negatively charged triplex DNA, cationic polycyclic compounds constitute the vast majority of known triplex-selective intercalators. On the other hand, positive charges at the intercalating moiety compromise binding to CG-rich sequences due to electrostatic repulsion with adjacent C^+·GC base triplets and consequently result in only weak stabilization of GC-rich targets in general.[32] However, third strand cytosines at the end of a triplex have been found to exhibit an apparent pK_a of about 5.5 and hence are expected to also be partly deprotonated at neutral pH at the triplex–duplex junction site.[33]

Optimized stacking interactions with base triplets are proposed to be major contributors to an intercalative mode of binding. To maximize those interactions, the overall shape of a triplex-selective polycyclic intercalator should closely match the crescent-shaped geometry of the three bases in a canonical base triad for an extensive overlap. Thus, the crescent-shaped B[*e*]PI and B[*g*]PI ligands are efficient triplex-stabilizing intercalators.[34] It is interesting to note, that the geometry of the four fused ring systems of our benzoannulated δ-carboline chromophore matches the shape of the B[*f*]PI ligand, that has previously been found to not significantly affect triplex stabilities at pH 6.2 with its more linear shape that does not match the shape of the base triplets (Fig. 6). Likewise, as expected from these simple geometric considerations, an indolo[3,2-*b*]-quinoline-11-carboxylic acid lacking a phenyl substituent and tethered through its carboxylic functionality to a third strand oligonucleotide binds duplex DNA with high affinity but failed to bind triplexes over duplexes with noticeable selectivity and affinity at pH 6.[35] Disregarding additional pH dependent effects, the considerable triplex stabilization of our δ-carboline ligand at low pH may therefore be attributed to the phenyl substituent at the tetracyclic ring system forming stacking interactions with the DNA bases. As an added benefit, the more flexible phenyl substituent might be better suited in maximizing stacking interactions with propeller-twisted base triads deviating from perfect planarity. Such a flexibility is often found to provide for an increased triplex stabilization of polycyclic compounds and has been exploited for the design of highly efficient triplex-selective intercalators.[13,23,36]

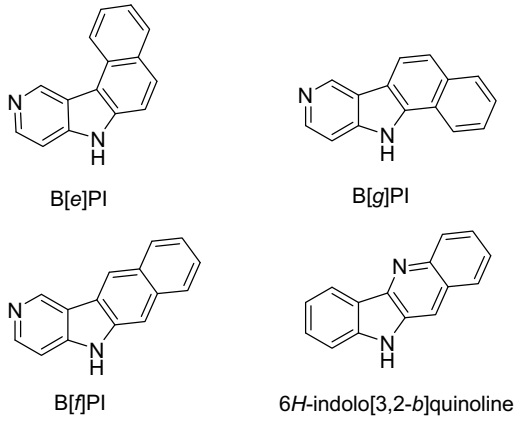

Figure 6. Chemical structures of benzopyridoindoles B[*e*]PI, B[*g*]PI and B[*f*]PI and the benzoannulated δ-carboline 6*H*-indolo[3,2-*b*]quinoline.

3. Conclusions

UV, CD and fluorescence data support well-defined interactions for the phenyl-substituted δ-carboline covalently attached to the TFO, resulting in a significant triplex thermal stabilization of up to $\Delta T_m = 23$ °C upon binding a duplex target. Given its efficient coupling to third strand oligonucleotides associated with the easy

availability of corresponding oligonucleotide conjugates, the δ-carboline moiety presented here seems to be a promising triplex binding ligand for a variety of potential applications. As an added advantage, the synthesis of this type of δ-carboline allows for a straightforward introduction of various substituents at different positions of the polycyclic compound and thus make the phenyl-substituted indoloquinoline a promising lead compound for the further development of this new class of triplex-selective intercalating agents. Clearly, for a better rational design more data on the pH dependence and sequence selectivity of δ-carbolines with appropriate triple-helical systems have to be collected in the future.

4. Experimental

4.1. Materials

Unmodified and 3′-amino modified oligonucleotides were purchased from *TIB MOLBIOL* (Berlin, Germany). The concentration was calculated using molar extinction coefficients at 260 nm derived from a nearest-neighbour model. The δ-carboline derivative 1,7-dimethyl-5-(4-carboxyphenyl)-6*H*-indolo[3,2-*b*]quinoline **1** was prepared according to previously published procedures.[37] The concentration of δ-carboline-modified oligonucleotide was approximated by using the determined molar extinction coefficient of the free δ-carboline carboxy derivative **1** at 260 nm ε_{260} = 26,818 M^{-1} cm^{-1}.

Solvents were distilled using a rotary evaporator prior to use. Buffer solutions were prepared using deionized water (Millipore Simplicity 185). All reactions were monitored by TLC using *Merck* silica gel plates $60F_{254}$. Silicagel (0.063–0.2 mm, *Mallinckrodt Baker*, The Netherlands) was used for normal column chromatography. For purifications through flash chromatography, a Yamazen AI-580 system (*Yamazen*, Osaka, Japan) equipped with a UV-detector at a fixed wavelength (254 nm) and with prepacked flash chromatography columns from Yamazen (Hi-Flash size L, Inject size M) was used. A mixture of methylene chloride and methanol in a ratio of 95:5 was employed for elution. HPLC separation was carried out with a Hitachi/Knauer system. The purification was performed on a reverse column (Kromasil 100 Å C18 5 μm, 4.6 × 250 mm, *Wicom GmbH*, Heppenheim, Germany). A gradient was applied using buffer A (0.1 M triethylammonium acetate/CH_3CN = 1:1, pH 6.8) and buffer B (0.1 M triethylammonium acetate/CH_3CN = 98:2, pH 6.8) as eluent. A flow rate of 1.2 mL/min was used and the fractions detected simultaneously at 260 nm, 281 nm, 347 nm and 406 nm. NMR spectra were recorded on a *Bruker* AVANCE 600 MHz spectrometer at room temperature.

4.1.1. 1,7-Dimethyl-5-(4-succinimidocarboxyphenyl)-6*H*-indolo[3,2-*b*]quinoline (2)

1,7-Dimethyl-5-(4-carboxyphenyl)-6*H*-indolo[3,2-*b*]quinoline **1** (112.7 mg, 0.3 mmol) was dissolved in DMF (4 mL). *N*-Hydroxysuccinimide (NHS, 95 mg) and *N*-(3-dimethylaminopropyl)-*N*′-ethylcarbodiimide hydrochloride (DCI, 157 mg) were added and the mixture was stirred for 2 days while monitored by TLC (CH_2Cl_2/CH_3OH 9:1). After completion, the solvent was removed under vacuo and the solid yellow residue dissolved in methylene chloride. It was washed three times with water and another three times with a concentrated solution of sodium chloride until the water phase was nearly colourless. The organic phase was dried using sodium sulfate and the solvent was removed by rotary evaporation. The product was finally purified by column chromatography and flash chromatography. Yield 130 mg (93%). ^{1}H NMR (600 MHz, CD_2Cl_2): δ(ppm) = 8.39 (d, *J* = 8.0 Hz, 2 H, ArH), 8.35 (d, *J* = 7.7 Hz, 1 H, ArH), 7.81 (d, *J* = 8.0 Hz, 2 H, ArH), 7.63 (d, *J* = 7.9 Hz, 1 H, ArH), 7.56 (d, *J* = 7.1 Hz, 1 H, ArH), 7.42 (d, *J* = 7.1 Hz, 1 H, ArH), 7.39 (t, *J* = 7.1 Hz, 1 H, ArH), 7.28 (t, *J* = 7.7 Hz, 1 H, ArH), 3.01 (s, 3 H, CH_3), 2.93 (s, 4 H, 2× CH_2), 2.51 (s, 3 H, CH_3).

4.1.2. Oligonucleotide-δ–carboline conjugate (3)

The 3′-amino-modified oligonucleotide (6.7 OD, 0.12 μmol) was dissolved in water (150 μL) and 0.1 M sodium phosphate buffer (pH 8.2, 65 μL) containing 50 mM lithium chloride was added. The NHS ester **2** (10 mg/ml, 2 μmol) dissolved in DMF (100 μL) was added and a yellow biphasic mixture was obtained. The solution was stirred for 5 days at 50 °C until the mixture became clear and checked by TLC (propanol/H_2O 5:3). The product mixture was dried under vacuo and the residue dissolved in water. Excessive NHS ester **2** was extracted three times by dichloromethane. The conjugate **3** was finally purified by HPLC and desalted by using Sep-Pak C18-Cartridges (*Waters Corporation*, Milford, USA). Yield 5.3 OD units (53%). MALDI-TOF-MS: *m/z* calcd for $C_{98}N_{30}O_{49}P_7H_{121}$: 2579.88. Found: 2578.51.

4.2. UV–vis spectroscopy

All UV measurements were performed on a *Cary 100* spectrophotometer equipped with a temperature control unit (*Varian* Deutschland, Darmstadt). Melting curves were recorded with 1 data point/°C at 260 nm in a temperature interval from 1 to 90 °C. To prevent water condensation on the cuvettes (1 cm path length) at temperatures below 25 °C, the sample chamber was constantly flushed with nitrogen gas. The lyophilized oligonucleotides (3.6 μM) were dissolved in cacodylate buffer pH 5.0 (0.02 M sodium cacodylate, 0.1 M NaCl, 0.001 M spermine) and annealed prior to each melting experiment by heating to 90 °C followed by slow cooling to room temperature. The third strand oligonucleotide or the conjugate was added to the duplex or complementary single strand in a ratio of about 1:1. Measurements included one heating ramp (1 °C/min), followed by one cooling (1 °C/min) and a second heating period (1 °C/min). Heating and cooling curves showed small hysteresis effects due to slow kinetics of 0.5–3 °C depending on the particular triplex. The melting temperature was determined by the maximum of the first derivative plot of the second heating curve after appropriate smoothing.

Titration experiments were performed by sequentially adding 10 aliquots of an oligonucleotide duplex solution to a 3.6 μM solution of the oligonucleotide conjugate to reach a final molar ratio of 2:1 without an appreciable change in total volume. Simultaneously, equal amounts of oligonucleotide were added to the reference cell to avoid large increases of DNA absorption during titration.

4.3. Circular dichroism

CD spectra were recorded with a Jasco J-810 spectropolarimeter (*Jasco*, Tokyo, Japan). Wavelength scans were acquired with 20 accumulations from 205 to 450 nm, a scanning speed of 50 nm/min, a response time of 8 s and a bandwidth of 1 nm. All CD experiments were carried out in cacodylate buffer pH 5.0 (0.02 M sodium cacodylate, 0.1 M NaCl, 0.001 M spermine) with a concentration of 8.2 μM of conjugate. The TFO conjugate was added to the duplex in a ratio of about 1:1.

4.4. Fluorescence measurements

Fluorescence measurements were performed with a Jasco FP-6500 spectrofluorometer (*Jasco*, Tokyo, Japan). Using an excitation wavelength of 350 nm, emission spectra from 360 to 600 nm were acquired with a scanning speed of 50 nm/min, an emission and excitation bandwidth of 5 nm and a response time of 0.1 s. To obtain a better *S/N* ratio five spectra were accumulated each. All fluorescence measurements were carried out in cacodylate buffer pH 5.0 (0.02 M

sodium cacodylate, 0.1 M NaCl, 0.001 M spermine) and a concentration of 2.2 μM of conjugate. The third strand oligonucleotide or the conjugate was added to the duplex in a ratio of about 1:1.

Acknowledgment

We thank Mrs. R. Schröder for her help in the synthesis of the δ-carboline derivatives.

References and notes

1. Hélène, C.; Thuong, N. T.; Harel-Bellan, A. *Ann. N.Y. Acad. Sci.* **1992**, *660*, 27–36.
2. Kim, H. G.; Miller, D. M. *Biochemistry* **1998**, *37*, 2666–2672.
3. Havre, P. A.; Gunther, E. J.; Gasparro, F. P.; Glazer, P. M. *Proc. Natl. Acad. Sci. U.S.A.* **1993**, *90*, 7879–7883.
4. Povsic, T. J.; Strobel, S. A.; Dervan, P. B. *J. Am. Chem. Soc.* **1992**, *114*, 5934–5941.
5. Perrouault, L.; Asseline, U.; Rivalle, C.; Thuong, N. T.; Bisagni, E.; Giovannangeli, C.; Le Doan, T.; Hélène, C. *Nature* **1990**, *344*, 358–360.
6. Strobel, S. A.; Doucette-Stamm, L. A.; Riba, L.; Housman, D. E.; Dervan, P. B. *Science* **1991**, *254*, 1639–1642.
7. Thuong, N. T.; Hélène, C. *Angew. Chem. Int. Ed. Engl.* **1993**, *32*, 666–690.
8. Fox, K. R. *Curr. Med. Chem.* **2000**, *7*, 17–37.
9. Sun, J.-S.; Francois, J.-C.; Montenay-Garestier, T.; Saison-Behmoaras, T.; Roig, V.; Thuong, N. T.; Hélène, C. *Proc. Natl. Acad. Sci. U.S.A.* **1989**, *86*, 9198–9202.
10. Silver, G. C.; Nguyen, C. H.; Boutorine, A. S.; Bisagni, E.; Garestier, T.; Hélène, C. *Bioconjugate Chem.* **1997**, *8*, 15–22.
11. Gianolio, D. A.; Segismundo, J. M.; McLaughlin, L. W. *Nucleic Acids Res.* **2000**, *28*, 2128–2134.
12. Jessen, C. H.; Pedersen, E. B. *Helv. Chim. Acta* **2004**, *87*, 2465–2471.
13. Filichev, V. V.; Pedersen, E. B. *J. Am. Chem. Soc.* **2005**, *127*, 14849–14858.
14. Géci, I.; Filichev, V. V.; Pedersen, E. B. *Bioconjugate Chem.* **2006**, *17*, 950–957.
15. Salunkhe, M.; Wu, T.; Letsinger, R. L. *J. Am. Chem. Soc.* **1992**, *114*, 8768–8772.
16. Letsinger, R. L.; Wu, T. *J. Am. Chem. Soc.* **1995**, *117*, 7323–7328.
17. Bevers, S.; Schutte, S.; McLaughlin, L. W. *J. Am. Chem. Soc.* **2000**, *122*, 5905–5915.
18. Lee, J. S.; Latimer, L. J. P.; Hampel, K. J. *Biochemistry* **1993**, *32*, 5591–5597.
19. Ihmels, H.; Otto, D.; Dall'Acqua, F.; Faccio, A.; Moro, S.; Viola, G. *J. Org. Chem.* **2006**, *71*, 8401–8411.
20. Mergny, J.-L.; Duval-Valentin, G.; Nguyen, C. H.; Perrouault, L.; Faucon, B.; Rougée, M.; Montenay-Garestier, T.; Bisagni, E.; Hélène, C. *Science* **1992**, *256*, 1681–1684.
21. Marchand, C.; Bailly, C.; Nguyen, C. H.; Bisagni, E.; Garestier, T.; Hélène, C.; Waring, M. J. *Biochemistry* **1996**, *35*, 5022–5032.
22. Baudoin, O.; Marchand, C.; Teulade-Fichou, M.-P.; Vigneron, J.-P.; Sun, J.-S.; Garestier, T.; Hélène, C.; Lehn, J.-M. *Chem. Eur. J.* **1998**, *4*, 1504–1508.
23. Wilson, W. D.; Tanious, F. A.; Mizan, S.; Yao, S.; Kiselyov, A. S.; Zon, G.; Strekowski, L. *Biochemistry* **1993**, *32*, 10614–10621.
24. Fox, K. R.; Polucci, P.; Jenkins, T. C.; Neidle, S. *Proc. Natl. Acad. Sci. U.S.A.* **1995**, *92*, 7887–7891.
25. Todorović, N.; Thi Bich Phuong, N.; Langer, P.; Weisz, K. *Bioorg. Med. Chem. Lett.* **2006**, *16*, 1647–1650.
26. Boulard, Y.; Gabarro-Arpa, J.; Cognet, J. A. H.; Le Bret, M.; Guy, A.; Téoule, R.; Guschlbauer, W.; Fazakerley, G. V. *Nucleic Acids Res.* **1991**, *19*, 5159–5167.
27. Chou, S.-H.; Tseng, Y.-Y.; Chu, B.-Y. *J. Biomol. NMR* **2000**, *17*, 1–16.
28. Manzini, G.; Xodo, L. E.; Gasparotto, D.; Quadrifoglio, F.; van der Marel, G. A.; van Boom, J. H. *J. Mol. Biol.* **1990**, *213*, 833–843.
29. Tuite, E.; Nordén, B. *J. Am. Chem. Soc.* **1994**, *116*, 7548–7556.
30. Bates, P. J.; Macaulay, V. M.; McLean, M. J.; Jenkins, T. C.; Reszka, A. P.; Laughton, C. A.; Neidle, S. *Nucleic Acids Res.* **1995**, *23*, 4283–4289.
31. Collier, D. A.; Mergny, J.-L.; Thuong, N. T.; Hélène, C. *Nucleic Acids Res.* **1991**, *19*, 4219–4224.
32. Keppler, M. D.; James, P. L.; Neidle, S.; Brown, T.; Fox, K. R. *Eur. J. Biochem.* **2003**, *270*, 4982–4992.
33. Leitner, D.; Schröder, W.; Weisz, K. *J. Am. Chem. Soc.* **1998**, *120*, 7123–7124.
34. Escudé, C.; Nguyen, C. H.; Mergny, J.-L.; Sun, J.-S.; Bisagni, E.; Garestier, T.; Hélène, C. *J. Am. Chem. Soc.* **1995**, *117*, 10212–10219.
35. Eritja, R. *Chem. Biodivers* **2004**, *1*, 289–295.
36. Gianolio, D. A.; McLaughlin, L. W. *Bioorg. Med. Chem.* **2001**, *9*, 2329–2334.
37. Langer, P.; Anders, J. T.; Weisz, K.; Jähnchen, J. *Chem. Eur. J.* **2003**, *9*, 3951–3964.